Sliding mode controller with fuzzy supervisor for MPPT of photovoltaic pumping system

Taleb Hamdi, Khaled Elleuch, Hafedh Abid, Ahmed Toumi

Laboratory of Sciences and Techniques of Automatic Control and Computer Engineering (Lab-STA), Department of Electrical Engineering, National School of Engineering of Sfax, University of Sfax, Sfax, Tunisia

Article Info

ABSTRACT

This paper focuses on a photovoltaic system for pumping water. The control strategy for this water pumping system is based on Takagi-Sugeno type fuzzy supervisors and sliding mode controller. The first generates the maximum power point current under varying climatic condition whereas the second allows tracking the reference signal produced by the fuzzy supervisor. The system includes a photovoltaic generator (PVG) followed by a DC-DC Converter, DC bus, an AC/DC inverter which is connected to the induction motor. This latter is coupled with a centrifuge pump. The induction motor is driven based on field-oriented control strategy. The Takagi-Sugeno type fuzzy supervisor predicts, depending on the variations of climatic variables such as irradiation and temperature, the optimum operating point for the photovoltaic source. The simulation results show the effectiveness of the proposed approach in transient and stationary regimes for different values of climatic variables.

Corresponding Author:

Taleb Hamdi
Laboratory of Sciences and Techniques of Automatic Control and Computer Engineering (Lab-STA)
Department of Electrical Engineering, National School of Engineering of Sfax, University of Sfax
Stax, Tunisia
Email: hamdi_taleb@hotmail.com

1. INTRODUCTION

In these last decades, the use of photovoltaic energy has grown rapidly due to its direct obtainability without causing pollution or noise. Referring to the studies that have been made by experts, solar energy is abundant in southern Tunisia, the average sunshine rate per day is around 7 kWh/m^2 in addition to 3200 hours of sunshine per year [1]. All of these have prompted leaders to think about "photovoltaic water". In Tunisia, the main reason delaying the use of photovoltaic technology for pumping water is a funding problem. However, an interesting program has been developed to exploit natural resources in particular the use of a photovoltaic generator for pumping water. The surface water resources are very limited, but deep-water resources are much more important. In addition, the majority of the population is settled around small villages with limited access to conventional energy sources; their water needs are relatively low and correspond to a moderate water consumption satisfying a certain household use. In reality, most type programs are supported by technical cooperation projects, in particular with Germany. For example, a photovoltaic micro-plant for pumping water for the irrigation of a palm grove of around 105 hectares has been installed in the Kebili region [2]. The project aims to install 14 photovoltaic pumps sponsored by the German Cooperation Agency (GIZ). In the literature, several works have been developed concerning the electric drive system best suited to water pumping applications with photovoltaic technology in the Saharan regions [3], [4].

Various works have been interested to PV water pumping system [5]–[7]. In this type of process, different kinds of motors have been used such as DC motors [8], brushless DC motor [9] and AC motors [10], [11], the choice depends on some factors such as the efficiency, the reliability and the price. However, water-pumping systems based on AC motors, particularly induction motors (IM), are more attractive because this type of motor is more robust than other types. They have high efficiency, easy maintenance, and low cost [3], [4]. Field oriented control (FOC) and direct torque control (DTC) are the most used control strategies for induction motor drives [12]. It is well known that FOC makes it possible to control the IM in a similar way to that of the direct current machine.

The performances of a PV micro-plant system depend on irradiation, temperature and type of load. However, maximum power point tracking (MPPT) has been used to maximize the extraction of power from the PV panels. In this context, several works are interested to the MPPT algorithms. There exist three big categories of MPPT algorithms, which are known as conventional methods, artificial intelligence and hybrid methods. Indeed, Mohammed *et al.* [13] presented perturb and observe (P&O) algorithm, the authors show that this method is simple to implement but the operating point remains oscillating around MPP and the operating point is not able to follow the maximum power point when there is a fast variation in environmental conditions. Kish *et al.* [14] presented the incremental conductance algorithm, this latest is simple for implementation and it converge rapidly. It is more efficient than P&O algorithm but the operating point oscillate around MPP. Chalok *et al.* [15] proposed an algorithm based on fuzzy logic to reduce the oscillations of the operating point but the implementation of the algorithm remains relatively complex. Idrissi *et al.* [16] neural network has been applied to track the maximum power point this algorithm provides rapid tracking and reduces oscillation but its complex for implementation.

The aim of this paper is to develop a new MPPT algorithm for an efficient PV water pumping system. The proposed algorithm is based on the combination of Takagi-Sugeno type fuzzy supervisor with sliding mode controller. From the climatic variables, essentially irradiation and temperature, the fuzzy supervisor is able to predict the coordinate of optimum operating point of the photovoltaic source as well as the maximum converted power. This power is used as a reference for a sliding mode controller to extract the maximum power from the panel and generate the duty cycle to the boost converter. The proposed controller guarantees good performance less oscillation and fast convergence to MPP. The power computed by the fuzzy supervisor is exploited to predict the reference speed of the induction motor, in order to control the flow rate of the pump.

The paper is organized as follows: Section 2 presents the block diagram description of the photovoltaic water pumping system; In the first part of section 3, the modeling of the photovoltaic panel is given; An MPPT algorithm, which results from the combination of sliding mode control with fuzzy systems, is given in the second part of section 3; In section 4, the different elements of the PV water pumping have been presented such as the voltage inverter, the induction machine operating under IFOC and the centrifugal pump; and In section 5, simulation results are given to illustrate the performance of the T-S fuzzy supervisor and the proposed approach. The paper is enclosed by concluding remarks.

2. DESCRIPTION OF THE PUMPING SYSTEM

The photovoltaic pumping station essentially comprises a source of photovoltaic energy, a DC/DC converter, followed by a DC bus connected to an inverter. The latter feeds an induction machine coupled to a water pump. An MPPT algorithm based on fuzzy logic and sliding mode is used to drive the DC/DC converter in order to extract the maximum power from the photovoltaic source. The induction machine is controlled according to the field-oriented control theory so that it behaves like a DC machine. The block diagram of the pumping process is shown by the Figure 1.
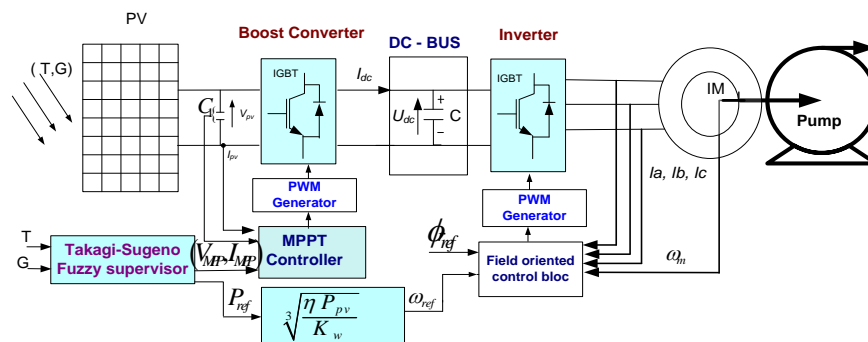

Figure 1. General diagram for a PV pumping system

3. PHOTOVOLTAIC PANEL MODEL AND MPPT CONTROLLER

This section includes two sub-sections. The first concerns the modelling of photovoltaic panel and DC/DC boost converter whereas, the second is reserved to the description of MPPT controller and fuzzy supervisor. The MPPT controller is basis on sliding mode and fuzzy system. The stability of system is verified by Lyapunov approach. Then the fuzzy supervisor is described to predict the optimal values of the main quantities of photovoltaic panel.

3.1. Modelling of photovoltaic panel and DC/DC converter

It is well known that the photovoltaic panel is obtained by a series-parallel assembly of a set of cells. Several mathematical models describe the evolution of the photovoltaic cell as a function of climatic parameters, mainly temperature and irradiation [17]. In this work, we adopt the model given by Figure 2.
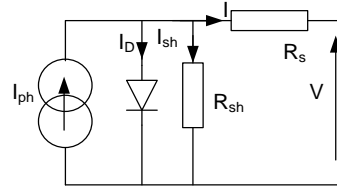

Figure 2. Equivalent electric model for a photovoltaic panel

The model of the photovoltaic panel is governed by (1)-(3).

$$I_{sh} = \frac{V + R_s I}{R_{sh}} \tag{1}$$

$$I = I_{ph} - I_0 \left[\exp\left(\frac{v + R_s I}{V_t}\right) - 1 \right] - \frac{(V + R_s I)}{R_{sh}} \tag{2}$$

$$V_t = \frac{n_s K T}{q} \tag{3}$$

The current produced by the photovoltaic panel changes according to the temperature and the irradiation in accordance with the expression described by (4):

$$I_{ph} = \left(I_{ph,n} + K_I \Delta T \right) \frac{G}{G_n} \tag{4}$$

$I_{ph,n}$ represents the nominal current supplied by the PV panel under standard climatic conditions of irradiation and temperature ($G = 1000$ w/m^2 and $T = 25$ °C).

$$I_0 = \frac{(I_{ph} + K_I \Delta T)}{\exp\left(\frac{V_{oc} + K_v \Delta T}{V_t}\right) - 1} \tag{5}$$

Where: I_0 is a reverse saturation current.

$$V_{oc} = n_s \frac{K T}{q} \log\left(\frac{I_{sc} + I_s}{I_s}\right) \tag{6}$$

$$V_c = n_s \frac{K T}{q} \log\left(\frac{I_{sc} + I_s - I_{pv}}{I_s}\right) \tag{7}$$

Where, V_{oc} represents the open circuit voltage and I_{sc} is the short circuit current. Figures 3 and 4 respectively display the evolution of the power characteristics as a function of the panel voltage following variations in irradiation and in temperature.

Before approaching the MPPT algorithm, it is crucial to introduce the modelling of the DC/DC converter. In fact, the main function of the DC/DC converter is to set the operating point by acting on the duty cycle μ, the variation range of which is limited between 0 and 1 ($0 \le \mu \le 0 C_{dc}$). In reality, there are several types of DC/DC converter such as boost, buck, buck-boost. The choice of converter is made according to the application. In this paper, we use a DC/DC Boost converter of which the structure is given by Figure 5. The mathematical model of the DC/DC boost converter is described by (8),

$$\begin{cases} \frac{dI_L}{dt} = -\frac{r_L}{L} I_L \big(V_{pv} - (1 - \mu)V_s \big) \\ \frac{dV_s}{dt} = \frac{1}{c_{dc}} \big((1 - \mu)I_L - I_{inv} \big) \end{cases} \qquad (8)$$

where r_L, L and C_2 represent respectively the resistance of the inductance, the inductance and the output capacitor.
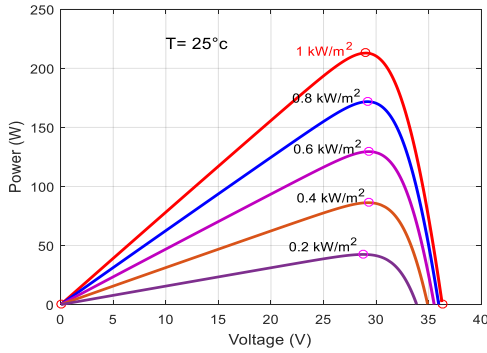

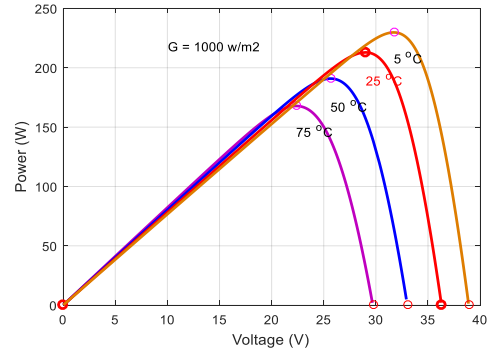Figure 3. Evolution of the power P (V) as a function of irradiation

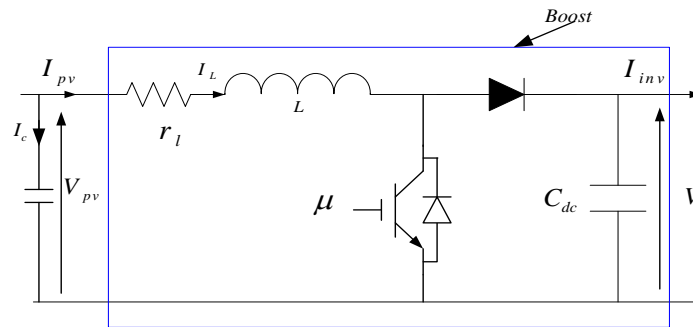Figure 4. Evolution of the power P (V) as a function of temperature

Figure 5. Structure of DC/DC boost converter

3.2. MPPT controller based on sliding mode and fuzzy supervisor

To extract the maximum power from PV panel, we propose a new MPPT algorithm that combines sliding mode and fuzzy logic techniques as displayed in Figure 6. The T-S Fuzzy supervisor provides optimum panel voltage and current, the sliding mode approach is employed to truck the reference current and provides the duty cycle, which will be transformed into a PWM signal.
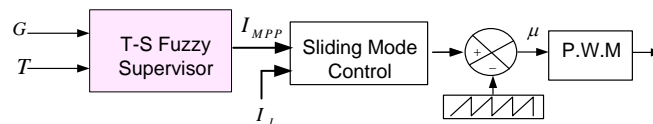

Figure 6. Block diagram of the MPPT algorithm

3.2.1. Sliding mode control

To extract the maximum power from the PV panel, we use a controller based on sliding mode to force the current to follow its reference value, which is computed by fuzzy supervisor. The output of controller generates the duty cycle μ to the boost converter. However, the sliding surface is defined by (9).

$$S = e_I + G \int e_I dt \qquad (9)$$

Where, G is a positive constant, $e_I = I_{MPP} - I_L$, I_{MPP} is the reference current at the output of the fuzzy logic supervisor. The derivative of the sliding surface is given by (10) and (11).

$$\dot{s} = Ge_I + \dot{e}_I \tag{10}$$

$$\dot{s} = Ge_I + \frac{r_L}{L}I_L\left(V_{pv} - (1-\mu)V_s\right) \tag{11}$$

Basis in the mode theories, the control law includes two terms. The first term is known as equivalent control law which is computed from $\dot{s} = 0$. Whereas the second term is known as switching control law which is expressed as: $Ksign\ (S)$.

$$\mu = \mu_{eq} + \mu_s \tag{12}$$

The expression of the equivalent control law, μ_{eq} is computed from $\dot{s} = 0$.

$$\dot{s} = Ge_I + \frac{r_L}{L}I_L\left(V_{pv} - \left(1-\mu_{eq}\right)V_s\right) = 0 \tag{13}$$

So,

$$\mu_{eq} = \left(1 - \frac{V_{pv}}{V_s}\right) + \frac{L}{V_s}\left(Ge_I + \frac{r_L}{L}I_L\right) \tag{14}$$

then,

$$\mu = \left(1 - \frac{V_{pv}}{V_s}\right) + \frac{L}{V_s}\left(Ge_I + \frac{r_L}{L}I_L\right) - Ksign\ (S) \tag{15}$$

To check the stability of the system, we use Lyapunov's theory. The candidate Lyapunov function is chosen as:

$$V = \frac{1}{2}S^2 \tag{16}$$

however, $\dot{V} = S\dot{S}$

$$\dot{V} = S\left[Ge_I + \frac{r_L}{L}I_L - \frac{1}{L}\left(V_{pv} - \left(1 - \left[\left(1 - \frac{V_{pv}}{V_S}\right) + \frac{L}{V_S}\left(Ge_I + \frac{r_L}{L}I_L\right) + Ksign\ (S)\right]\right)V_S\right)\right] \tag{17}$$

basis on (14) the last equation becomes as:

$$\dot{V} = S[-Ksign\ (S)] \tag{18}$$

$$\dot{V} = -K|S| < 0 \tag{19}$$

therefore, the stability of the system is guaranteed.

3.2.2. Fuzzy logic supervisor

The fuzzy systems are considered as universal approximators. They can consistently estimate all continuous functions defined in compact domains. Fuzzy techniques are able to convert nonlinear function into amalgamation of linear functions. The fuzzy system is described by an assembly of fuzzy rules whose structure is as follows [18], [19]:

$$if\ Z_1\ is\ M_{i1}\ and\ \ Z_2\ is\ M_{i2}\ and\ Z_n\ is\ M_{in}\ then\ y_1 = y_1^i, y_2 = y_2^i\ and\ y_3 = y_3^i \tag{20}$$

where, $\{M_{ij}\}$ describes the fuzzy sets, $Z_1(t) \dots Z_n(t)$ are the premise variables. $y(t) \in R_m$; c is the number of fuzzy rules. Each premise variable derives from a specific bounded domain such as: $Z_i(t)\epsilon[Z_{i\ min}Z_{i\ max}]$.

For each rule R_i, a weight $w_i\left(z(t)\right)$ is given which depends on score of membership function of premise variables $z_j(t)$ in fuzzy sets M_{ij}.

$$w_i\left(z(t)\right) = \prod_{j=1}^{n} M_{ij}\left(z_j(t)\right);\ w_i\left(z(t)\right) > 0;\ for\ i = 1, \dots c;$$

$M_{ij}\left(z_j(t)\right)$ is the score of membership of $z_j(t)$ to the fuzzy set M_{ij}.

$$h_i\big(z(t)\big) = \frac{w_i\big(z(t)\big)}{\sum_{i=1}^{c} w_i\big(z(t)\big)}; 0 < h_i\big(z(t)\big) < 1; i = 1, \dots c$$

The output of the fuzzy system is expressed as (21).

$$y_i(t) = \frac{\sum_{i=1}^{c} y_i^{j} \prod_{i=1}^{n} M_{ij}(Z_i)}{\sum_{j=1}^{c} \prod_{i=1}^{n} M_{ij}(Z_i)} \tag{21}$$

In this context, we have exploited a T-S type fuzzy supervisor given in Figure 7. The latter allows to predict in function of climatic variables, such as irradiation and temperature, the optimal values of the main quantities such as voltage V_{pv-ref}, current I_{MPP} and power p_{ref}. Figure 8 shows the membership function of irradiation as displayed which has two subsets M_{11} and M_{12}. The membership function for temperature as shown in Figure 9 is chosen with tow subsets M_{21} and M_{22}.
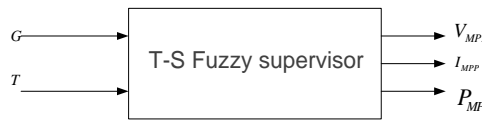
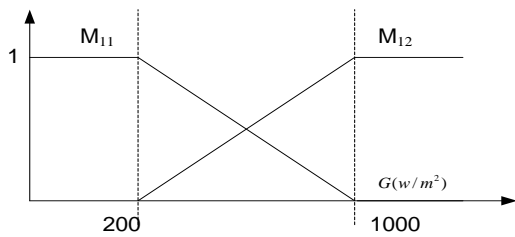Figure 7. T-S fuzzy supervisor

Figure 8. Member ship functions for irradiation   Figure 9. Member ship functions for temperature
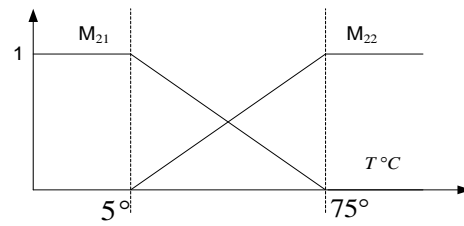
However, the T-S Fuzzy model of PV panel is well defined by the four following fuzzy rules: $y_{1i} = V_{MPPi} y_{2i} = I_{MPPi}, y_{3i} = P_{MPi}$ (for $i = 1$ to 4)

Plant rules:

Rule 1: $if\ Z_1$ is M_{11} and Z_2 is M_{21} then $V_{MPP} = V_{MPP1}, I_{MPP} = I_{MPP1}$ and $P = P_{MP1}$

Rule 2: $if\ Z_1$ is M_{12} and Z_2 is M_{21} then $V_{MPP} = V_{MPP2}, I_{MPP} = I_{MPP2}$ and $P = P_{MP2}$

Rule 3: $if\ Z_1$ is M_{11} and Z_2 is M_{22} then $V_{MPP} = V_{MPP3}, I_{MPP} = I_{MPP2}$ and $P = P_{MP2}$

Rule 3: $if\ Z_1$ is M_{12} and Z_2 is M_{22} then $V_{MPP} = V_{MPP4}, I_{MPP} = I_{MPP4}$ and $P = P_{MP4}$

Were,

$$M_{11}(z_2(t)) = \frac{Z_1(t) - Z_{1min}}{Z_{1max} - Z_{1min}} \quad M_{21}(z_2(t)) = \frac{Z_2(t) - Z_{2min}}{Z_{2max} - Z_{2min}}$$
$$M_{12}(z_1(t)) = \frac{Z_{1max}(t) - Z_1(t)}{Z_{1max} - Z_{1min}} \quad M_{22}(z_2(t)) = \frac{Z_{2max}(t) - Z_2(t)}{Z_{2max} - Z_{2min}}$$

So, the optimum voltage, current and power for a photovoltaic panel can be estimated by the following:

$$V_{MPP} = \sum_{i=1}^{c} h_i\big(z(t)\big) V_{MPPi} \tag{22}$$

$$I_{MPP} = \sum_{i=1}^{c} h_i\big(z(t)\big) I_{MPPi} \tag{23}$$

$$P_{max} = P_{MP} = \sum_{i=1}^{c} h_i\big(z(t)\big) P_{MPi} \tag{24}$$

4.   EQUIPMENT OF THE PUMP THROUGH THE DC BUS

After the DC/DC boost converter, the pumping chain comprises a DC bus, which feeds an induction motor through a three-phase inverter. The objective is to control the flow rate of the pump, which is a function of the rotational speed of the induction motor. This leads us to control the rotational speed of the motor. In this context, the field-oriented control technique is used to overcome the difficulties presented by the nonlinearities of the induction motor.

4.1. Voltage source inverter

The structure of the inverter, which consists of six IGBT switches, is shown in Figure 10. It is controlled by analogue PWM-type functions. The mathematical model of the inverter is given by (25).

$$\begin{bmatrix} V_a \\ V_b \\ V_c \end{bmatrix} = \frac{V_{dc}}{3} \begin{bmatrix} 2 & -1 & -1 \\ -1 & 2 & -1 \\ -1 & -1 & 2 \end{bmatrix} \begin{bmatrix} S_1 \\ S_2 \\ S_3 \end{bmatrix} \tag{25}$$

Where $S_1, S_2, S_3, \bar{S}_1, \bar{S}_2$ and $\bar{S}_3$ are the IGBT control signals and U_{dc} is the input DC voltage.
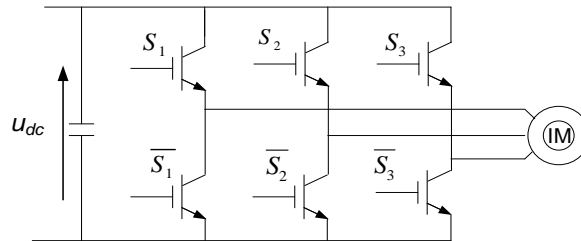

Figure 10. Structure of the inverter

4.2. Induction Motor model and field-oriented control

The state model of the induction machine in the (d, q) rotating frame is given by the following [20]:

$$\begin{cases} \dot{x}_1 = -\gamma\, x_1 + w_s\, x_1 + \frac{k}{T_r}\, x_3 + p\, k\ x_4\, x_5 + \frac{1}{\sigma\, L_s}\, v_{ds} \\ \dot{x}_2 = w_s\, x_1 + \gamma\, x_2 + \frac{k}{T_r}\, x_4 - p\, k\ x_3\, x_5 + \frac{1}{\sigma\, L_s}\, v_{qs} \\ \qquad \dot{x}_3 = \frac{M_{sr}}{T_r} x_1 - \frac{1}{T_r}\, x_3 + (w_s - p\, x_5)x_4 \\ \qquad \dot{x}_4 = \frac{M_{sr}}{T_r} x_2 - \frac{1}{T_r}\, x_4 - (w_s - p\, x_5)x_3 \\ \qquad \dot{x}_5 = \frac{1}{J} C_{em} - C_r \frac{1}{J} - \frac{f}{J}\, x_5 \end{cases} \tag{26}$$

where, w represents the Mechanical speed, $k = \frac{M_{sr}}{\sigma L_r L_s}$; $\gamma = \frac{R_s}{\sigma L_s} + \frac{R_r}{\sigma L_s L_r^2} M_{sr}^2\, T_r = \frac{L_r}{R_r}$; and

$$\sigma = 1 - \frac{M_{sr}^2}{L_r L_s} [x_1 \quad x_2 \quad x_3 \quad x_4 \quad x_5]^T = \begin{bmatrix} i_{ds} & i_{qs} & \emptyset_{dr} & \emptyset_{qr} & w \end{bmatrix}^T.$$

The expression of the electromagnetic torque is given by (27).

$$C_{em} = \frac{3}{2} \frac{p M_{sr}}{L_r} (x_2 x_3 - x_1 x_4) \tag{27}$$

The reference state model of the induction machine is based on the field-oriented control. It is well known that the principle of field control for the induction machine consists of keeping the rotor flux constant along the direct axis and cancelling the component of the flux along the quadrature axis [21], [22].

$$\emptyset_{dr} = cte \tag{28}$$

$$\emptyset_{qr} = 0 \tag{29}$$

The reference state model of the induction machine under the effect of field-oriented control becomes as (30).

$$\begin{cases} \dot{x}_1 = -\gamma\, x_1 + w_s\, x_2 + \dfrac{k}{T_r}\, x_3 + \dfrac{1}{\sigma\, L_s}\, v_{ds} \\ \dot{x}_2 = -w_s\, x_1 + \gamma\, x_2 - p\, k\ x_3\, x_5 + \dfrac{1}{\sigma\, L_s}\, v_{qs} \\ \qquad \dot{x}_3 = \dfrac{M_{sr}}{T_r} x_1 - \dfrac{1}{T_r}\, x_3 \\ \quad \dot{x}_4 = 0 = \dfrac{M_{sr}}{T_r} x_2 - (\, w_s - p\, x_5) x_3 \\ \qquad \dot{x}_5 = \dfrac{1}{J}\, \Gamma_{em} - C_r \dfrac{1}{J} - \dfrac{f}{j}\, x_5 \end{cases} \tag{30}$$

The expression of the electromagnetic torque becomes as (31). In this work, the goal is to control the speed of the motor, in the sense of controlling the flow of the pump.

$$\Gamma_{em} = \frac{3}{2} \frac{p M_{sr}}{L_r} (x_2 x_3) = K_e I_{qs} \emptyset_{dr} = K_{em} I_{qs} \tag{31}$$

Based on the reference power and the torque of pump we can deduce the optimum rotation speed of the induction motor. The useful power of the induction motor can be written as (32).

$$P_u = \Gamma_{em} w \tag{32}$$

We note η the efficiency of the pump motor assembly. It is defined by (33).

$$\eta = \frac{P_u}{P_{pv}} \tag{33}$$

The torque of pump is expressed as (34) [23].

$$\Gamma_p = k_w w^2 \tag{34}$$

However, the rotational speed can be computed as (35).

$$w = \sqrt[3]{\frac{\eta P_{pv}}{k_w}} \tag{35}$$

4.3. Centrifugal pump model
The centrifugal pumps are widely used for water pumping applications because they are designed for high flow-rates and low or medium depths (10 to 100 m). The centrifugal pump is known by the head-flow rate $H(Q)$ characteristic curve which depends on the motor speed value as displayed in Figure 11 [24]. The flow is proportional to the rotational speed motor while the head manometric (HMT) pressure gauge is proportional to the square of the speed.

The characteristic of the flow head of a centrifugal pump may be approximated by a quadratic function using the Pfleider-Peterman model [25], in which the speed of the rotor w is considered as a parameter:

$$H_{MT} = a_1 w_r^2 - a_2 w_r Q - a_3 Q^2 \tag{36}$$

where a_1, a_2 and a_3 are parameters which characterize the pump and given in the technical sheet. The characteristic $H(Q)$ of the pipe can be described by (37).

$$H = H_g + K_p Q^2 \tag{37}$$

The HMT (Q) curve as shown in Figure 11, is a parabola. The point where the HMT (Q) curve meets the ordinate axis is the point at zero flow. This is the closed valve point or the bubbling point. The operating point of the pump is given by the intersection of the characteristic of the water pipe with that of the pump that depends on the speed of motor rotation.
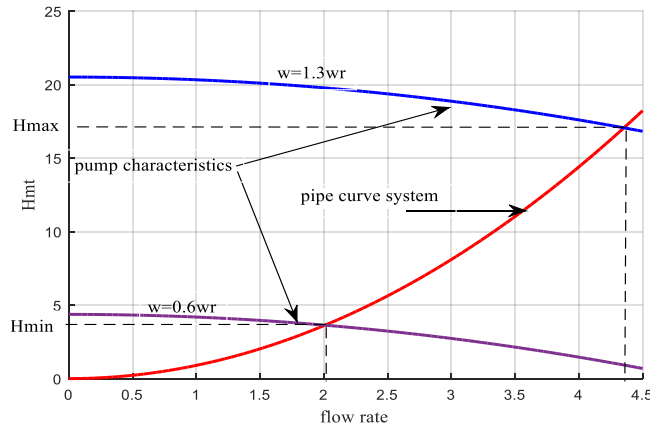
Figure 11. Characteristic of pump

5. SIMULATION RESULTS

The PV Generator used consists of twenty 1Soltech 1STH-215-P type photovoltaic panels. They are connected in two parallel strings; each one includes ten panels connected in serial. The boost converter parameters are chosen as $L = 10\ mH, R_L = 0.01\Omega, C_1 = 500\ \mu F\ and\ C_2 = 100\ \mu F$. The parameters of a panel are given in Table 1. The panel's fuzzy model consists of the following four local models:

i) $G=1000\ w/m^2, T = 5^0C, V_{MPP} = 31.71V, I_{MPP} = 7.2A, P = 229.75\ W$.
ii) $G=1000\ w/m^2, T = 75^0C, V_{MPP} = 22.35V, I_{MPP} = 7.5A, P = 167.8\ W$.
iii) $G=200\ w/m^2, T = 5^0C, V_{MPP} = 31.62V, I_{MPP} = 1.455A, P = 46\ W$.
iv) $G=200\ w/m^2, T = 75^0C, V_{MPP} = 21.74V, I_{MPP} = 1.513A, P = 32.892\ W$.

Table 1. Parameters for 1Soltech 1STH-215-P module

Parameters at 25 °C and 1000 w/m² for one panel	Nominal value
Maximum power P	213.15 W
Short circuit current I_{sc}	7.84 A
Open circuit voltage V_{co}	36.3 V
Optimal voltage	29 V
Optimal current	7.35 A

The variation of irradiation and temperature are given by the Figures 12 and 13. In the simulation, all losses are neglected and it is assumed that the efficiency of the motor pump is equal to unity $\eta=1$. The following Figures 14 to 20 show respectively the evolution of the power delivered by the photovoltaic panels, the actual and reference current in the inductance, the flux along the direct axis, the current along the d axis, the current along the q axis, the torque and the rotation speed of the induction motor.

Figures 12 and 13 show that the irradiation varied between 300 to 1000 and the temperature was kept constant. It is very logical that the power converted by the panels vary. When irradiation increases the power increases and vice versa. Figure 14 clearly appears that the inductance current follows its reference created by the supervisor by using the sliding mode control. Figure 16 shows that the field along the direct axis is constant. The Figure 17 appears that the current along the direct axis is constant. Figures 18 and 19 show respectively that the quadrature current and the torque are proportional. Figure 20 appears that the speed tracks the reference and varies smoothly as a function of the power supplied to the motor. Table 2 lists the induction motor parameters. Centrifugal pump parameters are:

$$w_n = 144\ rad/s, a_1 = 4.9234\ 10^{-4}\ m/(rad/s)^2\ , a_2 = 1.5826\ 10^{-5}\ m/(rad/s)^2\ (m^2/s),$$
$$a_3 = 0.18144\ m/(m^3/s)^2, k_p = 0.9, g = 9.81\ m^2/s,\ k_w = 4.4980e^{-04},\ \rho = 1000\ kg/m^3$$

Table 2. Induction motor parameters

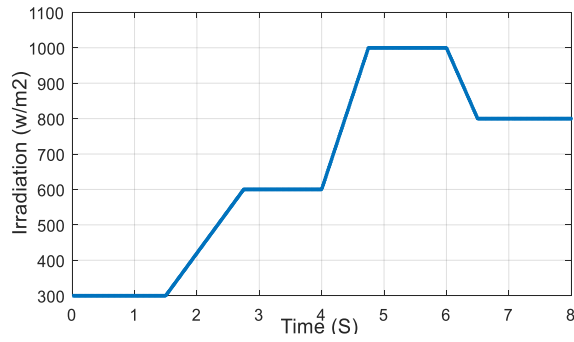| Parameters at 25 °C and 1000 w/m² for one panel	Nominal value	Parameters at 25 °C and 1000 w/m² for one panel	Nominal value
Maximum power P	4 KW	Mutual inductance	0.1722 H
Stator resistance R_s	1.405 Ω	Moment inertia	0.0131 kg.m²
Stator inductance L_s	5.839 mH	Friction	0.002985 rad/s
Rotor resistance R_r	1.395 Ω	Stator voltage	400 V
Rotor inductance L_r	5.839 mH	Frequency	50 Hz

Figure 12. Evolution of the irradiation
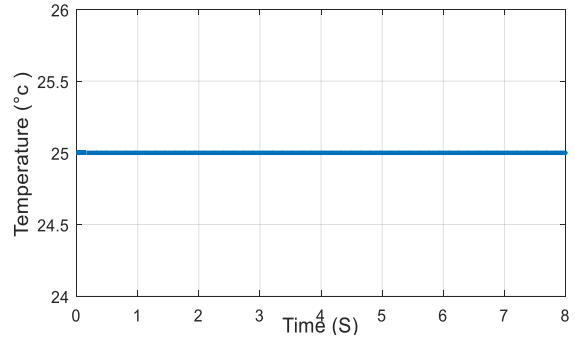
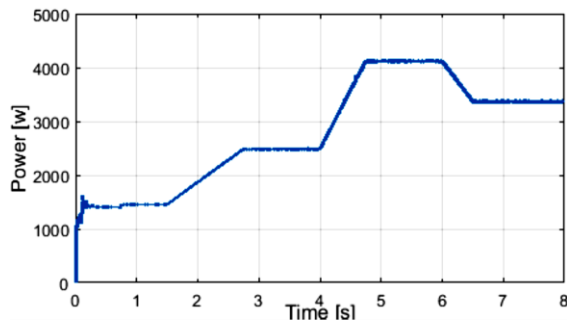Figure 13. Evolution of the temperature

Figure 14. Power converted By Photovoltaic panels
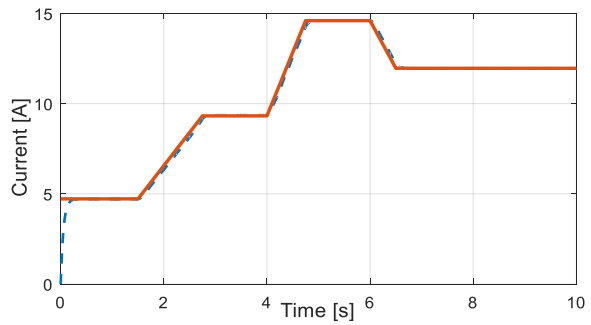

Figure 15. the actual and reference current in the inductance
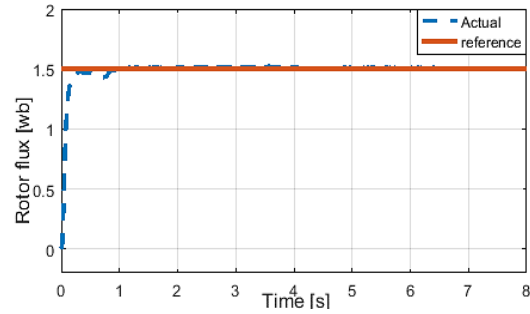

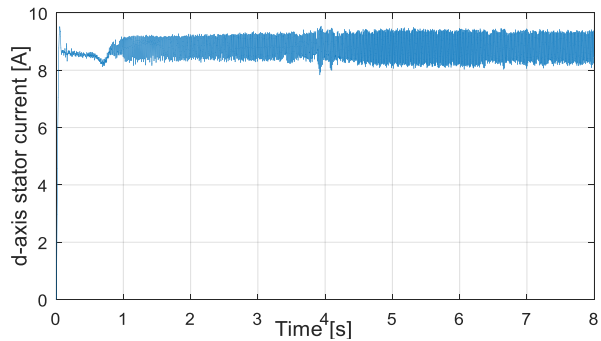
Figure 16. Flux along d axis
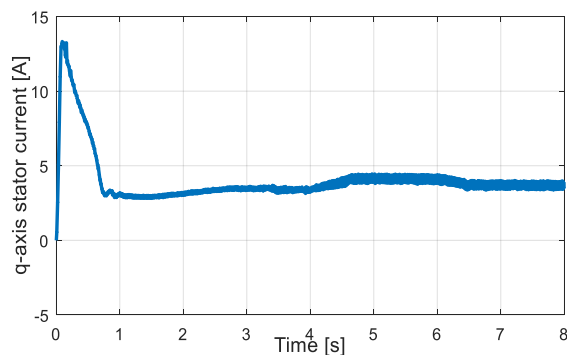

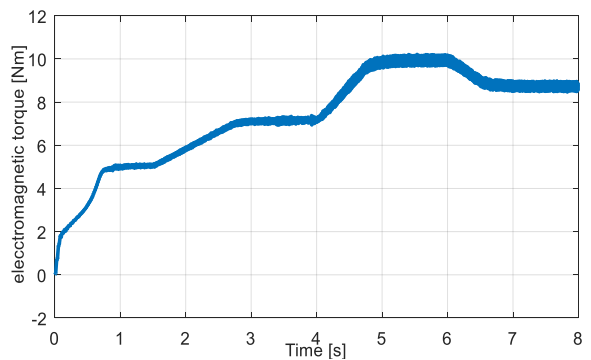Figure 17. Current along d axis
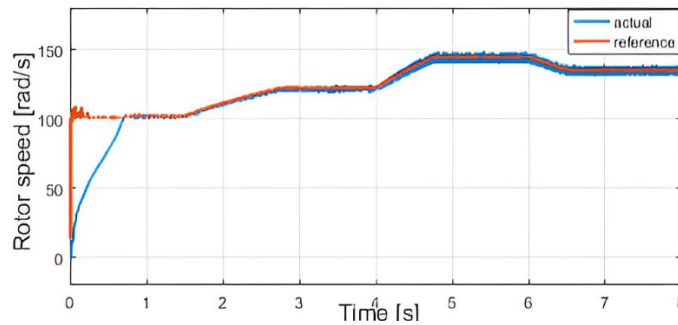

Figure 18. Current along q axis

Figure 19. Torque of induction motor

Figure 20. Motor speed

6. CONCLUSION

This paper deals with the optimal operation of a pumping system powered by a photovoltaic source using a pump coupled to an induction motor. Conventional and intelligent control techniques have been combined to ensure optimal system operation such as sliding mode control, field-oriented control and fuzzy systems. Climatic variables such as irradiation and temperature serve as inputs to the fuzzy supervisor which in turn provides the optimal values of the photovoltaic source which are current, voltage and power. The MPPT algorithm combines T-S fuzzy logic with sliding mode control techniques to extract the maximum energy from PV panels. The centrifugal pump is driven by an induction motor, which operates under field-oriented control. The flow of the pump varies according to the speed of rotation in a nonlinear way. At each speed of rotation, the pump has a well-defined flow rate. We use fuzzy systems to predict the reference speed of the induction motor and that of the pump according to the climatic variables temperature and irradiation which in turn make it possible to predict the reference power of the PV panels. The simulation results show the effectiveness of the proposed approaches.

REFERENCES

[1] N. El Ouanjli *et al.*, "Modern improvement techniques of direct torque control for induction motor drives - a review," *Protection and Control of Modern Power Systems*, vol. 4, no. 1, p. 11, Dec. 2019, doi: 10.1186/s41601-019-0125-5.

[2] I. M. Alsofyani and N. R. N. Idris, "A review on sensorless techniques for sustainable reliablity and efficient variable frequency drives of induction motors," *Renewable and Sustainable Energy Reviews*, vol. 24, pp. 111–121, Aug. 2013, doi: 10.1016/j.rser.2013.03.051.

[3] M. Errouha, A. Derouich, S. Motahhir, O. Zamzoum, N. El Ouanjli, and A. El Ghzizal, "Optimization and control of water pumping PV systems using fuzzy logic controller," *Energy Reports*, vol. 5, pp. 853–865, Nov. 2019, doi: 10.1016/j.egyr.2019.07.001.

[4] B. Talbi, F. Krim, T. Rekioua, S. Mekhilef, A. Laib, and A. Belaout, "A high-performance control scheme for photovoltaic pumping system under sudden irradiance and load changes," *Solar Energy*, vol. 159, pp. 353–368, Jan. 2018, doi: 10.1016/j.solener.2017.11.009.

[5] C. Gopal, M. Mohanraj, P. Chandramohan, and P. Chandrasekar, "Renewable energy source water pumping systems—A literature review," *Renewable and Sustainable Energy Reviews*, vol. 25, pp. 351–370, Sep. 2013, doi: 10.1016/j.rser.2013.04.012.

[6] D. H. Muhsen, T. Khatib, and F. Nagi, "A review of photovoltaic water pumping system designing methods, control strategies and field performance," *Renewable and Sustainable Energy Reviews*, vol. 68, pp. 70–86, Feb. 2017, doi: 10.1016/j.rser.2016.09.129.

[7] M. Errouha, A. Derouich, S. Motahhir, and O. Zamzoum, "Optimal Control of Induction Motor for Photovoltaic Water Pumping System," *Technology and Economics of Smart Grids and Sustainable Energy*, vol. 5, no. 1, p. 6, Dec. 2020, doi: 10.1007/s40866-020-0078-9.

[8] A. Yadav, A. Verma, P. K. Bhatnagar, and V. K. Jain, "Design of Photovoltaic System for DC Pumping Unit," in *Renewable Energy and Storage Devices for Sustainable Development*, 2022, pp. 147–153. doi: 10.1007/978-981-16-9280-2_18.

[9] A. Alice Hepzibah and K. Premkumar, "ANFIS current–voltage controlled MPPT algorithm for solar powered brushless DC motor based water pump," *Electrical Engineering*, vol. 102, no. 1, pp. 421–435, Mar. 2020, doi: 10.1007/s00202-019-00885-8.

[10] M. Errouha, A. Derouich, N. El Ouanjli, and S. Motahhir, "High-Performance Standalone Photovoltaic Water Pumping System Using Induction Motor," *International Journal of Photoenergy*, vol. 2020, pp. 1–13, Aug. 2020, doi: 10.1155/2020/3872529.

[11] R. L. Josephine, Y. Ganga Prasad Reddy, and B. P. Rachaputi, "Performance Analysis of Solar PV Array Fed Induction Motor Drive for Irrigation Applications," in *Lecture Notes in Electrical Engineering*, 2022, pp. 51–65. doi: 10.1007/978-981-16-7393-1_5.

[12] M. H. Holakooie, M. Ojaghi, and A. Taheri, "Direct Torque Control of Six-Phase Induction Motor With a Novel MRAS-Based Stator Resistance Estimator," *IEEE Transactions on Industrial Electronics*, vol. 65, no. 10, pp. 7685–7696, Oct. 2018, doi: 10.1109/TIE.2018.2807410.

[13] R. H. Mohammed, A. A. Abdulrazzaq, and W. K. Al-Azzawi, "Benefits of MPP tracking PV system using perturb and observe technique with boost converter," *International Journal of Power Electronics and Drive Systems (IJPEDS)*, vol. 13, no. 4, p. 2468, Dec. 2022, doi: 10.11591/ijpeds.v13.i4.pp2468-2477.

[14] G. J. Kish, J. J. Lee, and P. W. Lehn, "Modelling and control of photovoltaic panels utilising the incremental conductance method for maximum power point tracking," *IET Renewable Power Generation*, vol. 6, no. 4, p. 259, 2012, doi: 10.1049/iet-rpg.2011.0052.

[15] K. H. Chalok, M. F. N. Tajuddin, T. Sudhakar Babu, S. Md Ayob, and T. Sutikno, "Optimal extraction of photovoltaic energy using fuzzy logic control for maximum power point tracking technique," *International Journal of Power Electronics and Drive Systems (IJPEDS)*, vol. 11, no. 3, p. 1628, Sep. 2020, doi: 10.11591/ijpeds.v11.i3.pp1628-1639.

[16] Y. E. A. Idrissi, K. Assalaou, L. Elmahni, and E. Aitiaz, "New improved MPPT based on artificial neural network and PI controller for photovoltaic applications," *International Journal of Power Electronics and Drive Systems (IJPEDS)*, vol. 13, no. 3, p. 1791, Sep. 2022, doi: 10.11591/ijpeds.v13.i3.pp1791-1801.

[17]   M. A. Hasan and S. K. Parida, "An overview of solar photovoltaic panel modeling based on analytical and experimental viewpoint," *Renewable and Sustainable Energy Reviews*, vol. 60, pp. 75–83, Jul. 2016, doi: 10.1016/j.rser.2016.01.087.

[18]   J. J. Buckley, "Sugeno type controllers are universal controllers," *Fuzzy Sets and Systems*, vol. 53, no. 3, pp. 299–303, Feb. 1993, doi: 10.1016/0165-0114(93)90401-3.

[19]   H. Abid, M. Chtourou, and A. Toumi, "An indirect model reference robust fuzzy adaptive control for a class of SISO nonlinear systems," *International Journal of Control, Automation and Systems*, vol. 7, no. 6, pp. 982–991, Dec. 2009, doi: 10.1007/s12555-009-0615-8.

[20]   O. Asseu, M. Koffi, Z. Yeo, X. Lin-Shi, M. A. Kouacou, and T. J. Zoueu, "Robust Feedback linearization and Observation Approach for Control of an Induction Motor," *Asian Journal of Applied Sciences*, vol. 1, no. 1, pp. 59–69, Dec. 2007, doi: 10.3923/ajaps.2008.59.69.

[21]   F. Wang, Z. Zhang, X. Mei, J. Rodríguez, and R. Kennel, "Advanced Control Strategies of Induction Machine: Field Oriented Control, Direct Torque Control and Model Predictive Control," *Energies*, vol. 11, no. 1, p. 120, Jan. 2018, doi: 10.3390/en11010120.

[22]   H. Aziri, F. A. Patakor, M. Sulaiman, and Z. Salleh, "Comparison Performances of Indirect Field Oriented Control for Three-Phase Induction Motor Drives," *International Journal of Power Electronics and Drive Systems (IJPEDS)*, vol. 8, no. 4, p. 1682, Dec. 2017, doi: 10.11591/ijpeds.v8.i4.pp1682-1692.

[23]   K. Benlarbi, L. Mokrani, and M. S. Nait-Said, "A fuzzy global efficiency optimization of a photovoltaic water pumping system," *Solar Energy*, vol. 77, no. 2, pp. 203–216, 2004, doi: 10.1016/j.solener.2004.03.025.

[24]   A. Betka and A. Moussi, "Performance optimization of a photovoltaic induction motor pumping system," *Renewable Energy*, vol. 29, no. 14, pp. 2167–2181, Nov. 2004, doi: 10.1016/j.renene.2004.03.016.

[25]   A. Betka and A. Attali, "Optimization of a photovoltaic pumping system based on the optimal control theory," *Solar Energy*, vol. 84, no. 7, pp. 1273–1283, Jul. 2010, doi: 10.1016/j.solener.2010.04.004.

BIOGRAPHIES OF AUTHORS

Taleb Hamdi [ORCID] [GS] [SC] [web] obtained his Master degree in Automatic Control from Higher School of Sciences and Techniques of Tunis, Tunisia (E.S.S.T.T.) in 2009. Currently, he is a research member in Laboratory of Sciences and Techniques of Automatic & computer engineering (Lab-STA) in National Engineering School of Sfax, University of Sfax. He is currently pursuing PhD at the Department of Electrical Engineering. His research interests include sliding mode, control of linear and nonlinear systems and renewable energy. He can be contacted at email: hamdi_taleb@hotmail.com.

Khaled Elleuch [ORCID] [GS] [SC] [web] obtained the M.S degree on January 1996 in electrical engineering from the ESSTT of Tunis, Tunisia. He is member of Laboratory of Sciences and Techniques of Automatic & computer engineering (Lab-STA) in National Engineering School of Sfax, University of Sfax. He obtained the Ph.D degree from National Engineering School of Sfax ENIS, Tunisia on June 2010. Currently, he is an associate professor in the Higher Institute of Biotechnology of Sfax ISBS, Tunisia. His researches focus on identification and control of nonlinear systems, photovoltaic energy and wind energy. He can be contacted at email: Khaled.elleuche@isbs.usf.tn.

Hafedh Abid [ORCID] [GS] [SC] [web] had an electrical engineering diploma from the National School of Engineering of Sfax, Tunisia in 1989, then a diploma in Electrical and Electronic from the High School of Technical Sciences of Tunis in 1995 and in 1996 the Aggregation in Electric Genius. From 1996 to 2006, he was a 'Technologies' Teacher of the Electric Department in High Institute of Technology's of Sousse. He is working now as a Professor at National School of Engineering of Sfax, University of Sfax, Tunisia. His current research interests are fuzzy systems and photovoltaic systems. He is the author and co-author of numerous national and international publications. He can be contacted at email: hafedh.abid@enis.tn.

Ahmed Toumi [ORCID] [GS] [SC] [web] is an electrical engineer from the Sfax Engineering National School, he has the DEA in instrumentation and Measurement from University of Bordeaux, France in 1981 and the Thesis degree from the University of Tunis in 1985. He joined the National Engineering School as an Associate Professor, since 1981. In 2000, he had the University Habilitation (HDR) from the Engineering School of Sfax, Tunisia. He was working as a director of the Electrical Engineering Department in ENIS. Study and research areas touch modeling, stability of electric machines and electrical networks. He can be contacted at email: ahmed.toumi@enis.tn.